Water Research 202 (2021) 117427

Contents lists available at ScienceDirect

Water Research

journal homepage: www.elsevier.com/locate/watres

Characterizing 19 thousand Chinese lakes, ponds and reservoirs by morphometric, climate and sediment characteristics

Annette B.G. Janssen [a,*], Bram Droppers [a], Xiangzhen Kong [b,c], Sven Teurlincx [d], Yindong Tong [e], Carolien Kroeze [a]

[a] Water Systems and Global Change Group, Wageningen University & Research, PO Box 47, 6700 AA Wageningen, the Netherlands
[b] UFZ - Helmholtz Centre for Environmental Research, Department Lake Research, Brückstr. 3a, 39114 Magdeburg, Germany
[c] State Key Laboratory of Lake Science and Environment, Nanjing Institute of Geography & Limnology, Chinese Academy of Sciences, Nanjing, 210008, China
[d] Department of Aquatic Ecology, Netherlands Institute of Ecology (NIOO-KNAW), P.O. Box 50, 6700 AB Wageningen, the Netherlands
[e] School of Environmental Science and Engineering, Tianjin University, Tianjin 30000, China

ARTICLE INFO

Keywords:
Eutrophication
Algal blooms
Vulnerability
Stratification
VIC-LAKE
PCLake

ABSTRACT

Chinese lakes, including ponds and reservoirs, are increasingly threatened by algal blooms. Yet, each lake is unique, leading to large inter-lake variation in lake vulnerability to algal blooms. Here, we aim to assess the effects of unique lake characteristics on lake vulnerability to algal blooms. To this end, we built a novel and comprehensive database of lake morphometric, climate and sediment characteristics of 19,536 Chinese lakes, including ponds and reservoirs (>0.1 km^2). We assessed lake characteristics for nine stratification classes and show that lakes, including ponds and reservoirs, in eastern China typically have a warm stratification class (T_{avg}>4 °C) and are slightly deeper than those in western China. Model results for representative lakes suggest that the most vulnerable lakes to algal blooms are in eastern China where pollution levels are also highest. Our characterization provides an important baseline to inform policymakers in what regions lakes are potentially most vulnerable to algal blooms.

Introduction

Chinese lakes, including ponds and reservoirs, are of great economic, environmental and cultural importance (Chang et al., 2020; Huang et al., 2020) by providing the world's largest freshwater fish culture, facilitating drinking water and supporting tourism (Gao and Zhang 2010). China accommodates over 20% of the world's human population with only 0.5% of the world's lake volume spread over 6% of the global land surface area (Guan and Hubacek 2007; Messager et al., 2016, World Bank 2017). Lakes are thus considered a critical natural resource in large parts of the country (Guan and Hubacek 2007).

Many Chinese lakes are currently eutrophic, negatively impacting ecosystem services (Janssen et al., 2020; Liu et al., 2010), with the most pronounced examples of toxic algal blooms in Lake Taihu (Janssen et al., 2017; Wang et al., 2019), Lake Chaohu (Kong et al., 2016) and Lake Dianchi (Li et al., 2019). However, lakes show different levels of resilience to algal blooms, despite receiving similar amounts of nutrients (Janssen et al., 2014; Liu et al., 2010). Natural factors such as morphometric, climate and sediment characteristics could explain up to 58% of the variance in chlorophyll-a and are, therefore, considered as fundamental properties causing this inter-lake variability in vulnerability to algal blooms (Liu et al., 2010; Messager et al., 2016; Schäfer et al., 2014).

Morphometric lake characteristics are indicators of lake dimensions such as depth, lake area and shoreline development (i.e. a measure of shoreline irregularity defined as shoreline length over lake area). For instance, lake vulnerability to algal blooms is affected by the depth, which increases the nutrient buffer capacity (Liu et al., 2010; Qin et al., 2020), the lake area, which increases wind-induced resuspension (Evans 1994; Scheffer 2004) and, shoreline development, which creates wind-shelters for macrophytes (Andersson 2001; Aronow 1984; Janssen et al., 2014). Climate characteristics are long-term meteorological conditions such as ice periods and water temperature in the epilimnion and hypolimnion. For example, climate conditions affect the vulnerability to algal blooms by driving the timing of mixing and stratification of lakes and thereby determining nutrient losses and release processes (Janssen et al., 2019b; Qin et al., 2020). Sediment characteristics are indicators of the bottom materials of lakes such as sediment density and clay and sand

* Corresponding author.
E-mail address: annette.janssen@wur.nl (A.B.G. Janssen).

https://doi.org/10.1016/j.watres.2021.117427
Received 23 February 2021; Received in revised form 29 June 2021; Accepted 5 July 2021
Available online 10 July 2021

content. Sediment characteristics affect the vulnerability to algal blooms by regulating the phosphorus mobility and resuspension processes in lakes (Søndergaard et al., 2003).

Here, we aim to assess the effects of unique lake characteristics on lake vulnerability to algal blooms. We assessed 19,536 lakes larger than 0.1 km^2, including (glacial) ponds and reservoirs in mainland China (Fig. 1) extracted from HydroLAKES (Messager et al., 2016). First, we group the lakes based on their stratification classes and analyze the spatial variabilities of these stratification classes. Next, we study how lake morphometric, climate and sediment characteristics vary among the stratification classes. Finally, we simulate the effect of typical lake characteristics per stratification class on the vulnerability of lakes to algal blooms. We define vulnerability as the possibility of being harmed by algal blooms when being exposed to stress from nutrient pollution. A lake can thus be highly vulnerable, yet if the nutrient pollution remains sufficiently low, algal blooms will not occur. Our characterization provides an important baseline to inform policymakers in what regions lakes are potentially most vulnerable to algal blooms.

Methods

In our analysis we 1) group lakes into stratification classes to determine how these classes are spatially distributed, 2) identify the morphometric, climate and sediment characteristics to assess the variation in lake characteristics among stratification classes, and 3) assess the lake vulnerability to algal blooms for representative lakes each reflecting a stratification class. Below we describe the methods for these steps.

Data collection of lake characteristics

Morphometric characteristics

To study the lake morphometric characteristics we included lake area, depth and shoreline development (a measure of lake shape, calculated as a ratio between shoreline length and circumference of a circle with the same area) from the HydroLAKES database developed by Messager et al. (2016). The HydroLAKES database is considered the most complete database of lakes around the world. The morphometric characteristics are provided with acceptable ranges for uncertainty yet with a better predictive power for larger lakes than smaller lakes (Messager et al., 2016). The HydroLAKES database is based on seven different databases (CanVec, SWBD, MODIS, NHD, ECRINS, GLWD and GRanD) that used radar technology, long-term imagery composites and topographic maps to extract polygons of individual lakes with a surface area larger than 0.1 km^2. The extracted polygons are post-processed by Messager et al. (2016) for quality assurance. Lake area and shoreline development followed from, respectively, the surface area and circumference of the final set of polygons. Messager et al. (2016) calculated average lake depth using an elevation model validated on 5000 lakes combined with elevation data from EarthEnv-DEM90 (Robinson et al., 2014). To study the morphometric characteristics we selected the lakes from the HydroLAKES database located in mainland China.

Climate characteristics

For the lake climate characteristics, we used the VIC-LAKE model (Bowling and Lettenmaier 2010) to simulate the daily 1D temperature profile for every single lake within the set of lakes selected from HydroLakes. VIC-LAKE is a 1-dimensional lake temperature model (Bowling and Lettenmaier 2010) and is based on seminal work on the

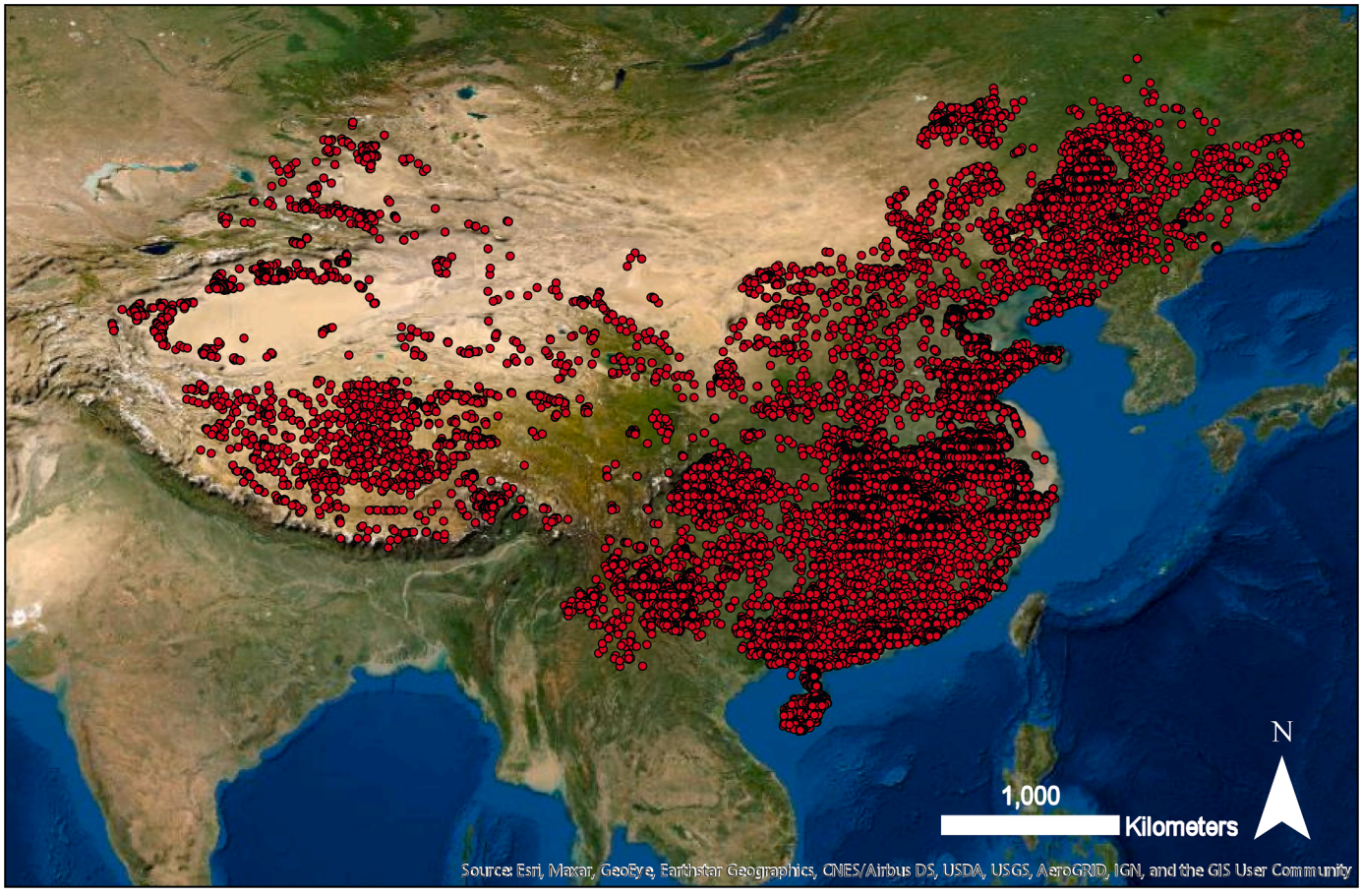

Fig. 1. Locations of lakes, including (glacial) ponds and reservoirs, in mainland China. Basemap from the Environmental Systems Research Institute (ESRI 2021).

lake energy balance by Hostetler and Bartlein (1990), Hostetler (1991) and Patterson and Hamblin (1988). Previous studies have used VIC-LAKE to simulate water temperatures and ice-cover for a variety of lakes (Bowling and Lettenmaier 2010; Mishra et al., 2011) and the model has been used in ISIMIP (Inter-Sectoral Impact Model Intercomparison Project) for climate impact studies on lakes (ISIMIP 2020). We ran VIC-LAKE to simulate water temperature for the period 1900–2005 with 0.5 m depth temperature intervals. As input we used climate forcing (1900–2005) from four climate models from ISIMIP: GFDL-ESM2M, HadGEM2-ES, IPSL-CM5A-LR and MIROC5. This climate data are available on a 0.5°x0.5° lat-long grid and includes air temperature, precipitation, atmospheric pressure, incoming short and longwave radiation, vapor pressure and wind speed. We simulated the lake temperature for each lake using the climate forcing of the grid that coincided with the lake's pour point location (i.e. lake outlet) as provided by HydroLAKES. All temperatures were height-corrected to adjust for lower temperatures at higher elevation using a fixed lapse rate of 6.5 °C km^{-1}. We used the first 100 years of our run (1900–2000) for analysis on the baseline conditions of the climate characteristics.

A common approach to evaluate model performance is to regress predicted (x-axis) versus observed values (y-axis) and compare intercept and slope parameters against the 1:1 line (Piñeiro et al., 2008). An intercept close to 0 and a slope close to 1 reflects a good fit. Here, we used the linear model function ('lm') of the 'stats' package in R to find the linear regression lines between modelled (VIC- LAKE output) versus observed (MODIS), resulting in 5 regression lines (4 with VIC-LAKE output generated with the 4 climate models and the last for the model average). Each regression line was plotted against surface water temperature observations of MODIS for 216 Chinese lakes from the Land Processes Distributed Active Archive Center (LP DAAC 2020). In our analysis, we excluded the modelled output during ice-coverage periods, because there is a mismatch in surface temperature between VIC-LAKE, which is predicted just below the ice-layer, and the data from MODIS which provides the temperature on top of the ice-layer. Besides a general validation, we also included some exemplary time series of individual lakes in Appendix A to compare the seasonal patterns of VIC-LAKE with data.

Sediment characteristics

To study the lake sediment characteristics we used estimations from soil maps. Most soil maps have data on terrestrial systems while lacking the data of aquatic systems. Since lakes are depressions in the landscape that collect eroded top-soil from their surroundings, we assumed that the most common sediment type around the lake corresponds with the sediment type in the lake. We used the shapefiles of the Chinese lakes provided by the HydroLAKES database (Messager et al., 2016) in combination with the Harmonized World Soil Database (FAO/IIASA/ISRIC/ISS-CAS/JRC 2009) to estimate lake sediment characteristics. We drew a buffer of 1000 meter around the HydroLAKES shapefiles and applied zonal statistics on this buffer to find the most common sediment type around the lake. The same method for a set of European lakes resulted in about 71% of the cases in an acceptable classification (Appendix B).

Grouping lakes by stratification classes

The stratification class of a lake depends on the number and duration of stratification periods and ice-coverage. Following the limnologic stratification classification system, lakes can be classified as *amictic* lakes that are continuously ice-covered, *continuous polymictic* lakes that are continuously mixed, *discontinuous polymictic lakes* that occasionally stratify each year, *monomictic* lakes that stratify once a year for a longer period, *dimictic* lakes that stratify twice a year for a longer period, and *meromictic* lakes that are continuously stratified (Lewis Jr 1983; Woolway and Merchant 2019). Within this classification, lakes can be distinguished by warm lake classes (yearly average surface water temperature >4 °C) and cold lake classes (yearly average surface water temperature <4 °C). Warm lake classes are 1) *polymictic continuous warm* lakes, 2) *polymictic discontinuous warm* lakes, 3) *monomictic warm* lakes, 4) *dimictic* lakes and 5) *meromictic* lakes. Cold lake classes are 6) *polymictic continuous cold* lakes, 7) *polymictic discontinuous cold* lakes, 8) *monomictic cold* lakes and 9) *amictic* lakes.

To determine the reference stratification classification of each lake we used the simulated outcomes of the VIC-LAKE model for water temperature and ice-period for the period 1900–2000 to estimate the period of stratification. To do so, we first calculated the water density (ρ_d,[$kg.m^{-3}$]) based on the simulated water temperature (T_d,[°C]) at each depth (d, [m]), following the ISIMIP protocol (Bigg 1967; Millero and Poisson 1981):

$$\rho_d = 999.842594 + (6.793952\times10\text{–}2 \text{ x } T_d) - (9.095290 * 10\text{–}3 \text{ x } T_d^2) + (1.001685\times10\text{–}4 \text{ x } T_d^3) - (1.120083\times10\text{–}6 \text{ x } T_d^4) + (6.536336\times10\text{–}9 T_d^5)$$

Next, the water density gradient ($\Delta\rho_d$) was calculated as:

$$\Delta\rho_{d=}\rho_d - \rho_{d-1}$$

The depth of the steepest density gradient is taken as the boundary between the epilimnion and the hypolimnion.

For each day of the year, we averaged both the epilimnion and the hypolimnion temperatures to obtain a 100-year averaged time series of the epilimnion and the hypolimnion temperatures. When density differences between the epilimnion and hypolimnion exceeded 0.1 kg m^{-3} we defined the lake as being stratified. Based on the number and duration of the stratification periods, the stratification class for each lake has been determined.

We chose to exclude salt lakes and fully frozen lakes from our analysis as their characteristics interfere with the thermal stratification dynamics studied here. Salt lakes can exhibit chemical stratification and are typically endorheic, meaning that there is no outflow. Hence, evaporation is larger than the dilution by inflowing rivers or precipitation. To our knowledge, a comprehensive overview of Chinese salt lakes is not available. Therefore, we decided to define all lakes for which the evaporation was larger than the sum of the water inflow and precipitation as salt lakes. Lakes frozen entirely from the surface to the bottom cannot be thermally stratified, as liquid water is required. Lakes for which VIC-LAKE predicted a full-frozen lake were characterized as such and, together with salt lakes, were excluded from our classification and subsequent analyses.

Spatial and statistical analysis

Globally, lake stratification classes typically follow the north-south axis. Yet for the analysis of lakes in China, we divided lakes into east and west lakes following the country's two geographically distinct climate regions roughly divided by the Hu Huanyong Line: a mountainous and temperate continental climate to the west and a (sub)tropical monsoon climate to the east. Next, to assess whether the Chinese lakes follow the global north-south patterns, we translocated the lakes by calculating the altitude corrected latitude ('adjusted latitude') following Lewis Jr (1983) (Appendix C).

For each stratification class, we calculated the statistical variation within the different lake characteristics. Since our data were not normally distributed we used an asymptotic K-Sample Fisher-Pitman Permutation Test with the function 'oneway_test' of the 'coin' library in R (Hothorn et al., 2019) to test whether groups of stratification classes are equal to randomly selected groups of lakes. A global p-value < 0.05 indicates that the stratification classes are not equal to randomly chosen lakes from the entire data set and thus that lake characteristics are unique for each stratification class. Next, we used a Pairwise K-sample permutation test with the function 'pairwisePermutationMatrix' of the 'rcompanion' in R (Mangiafico and Mangiafico 2017) to conduct permutation tests across groups.

Simulating vulnerability of lakes to algal blooms

As a final step, we assessed the lake vulnerability to algal blooms for each of the stratification classes. Lake vulnerability is expressed by two indicators:

1) The possible severity of algal blooms expressed here as the maximum chlorophyll-a concentration that could emerge in the epilimnion (red line Fig. 2);
2) The possible onset of algal blooms expressed as the critical nutrient load, which is the amount of nutrient load at which the yearly average epilimnion algal concentrations exceed 20 $\mu g.l^{-1}$ (Carlson 1977) (blue line Fig. 2).

We assessed the lake vulnerability to algal blooms for 9 representative lakes, each reflecting a stratification-class with its specific morphometric, climate and sediment characteristics through bifurcation analyses using the dynamic ecosystem model PCLake+ (Janssen et al., 2019b). A bifurcation analysis is a technique to study the effect of external pressure (here phosphorus load) on the water quality state (here chlorophyll-a). PCLake+ has been successfully applied for numerous lakes including the Chinese lakes Taihu (Janssen et al., 2017), Chaohu (Kong et al., 2016) and Dianchi (Li et al., 2019).

A bifurcation analysis results in two load-response curves (x-axis: P-load, y-axis: chlorophyll-a), one for the process of eutrophication (clear–>turbid) and one for oligotrophication (turbid–>clear) (Fig. 2). The vulnerability in terms of the possible severity of algal blooms is measured as the maximum chlorophyll-a level within the load-response curves, which is reached when algae become light-limited (Chang et al., 2019). The vulnerability in terms of the onset of algal blooms is measured as the critical nutrient load ($gP.m^{-2}.d^{-1}$) at which the load-response graph crosses the chlorophyll-a concentration of 20 $\mu g.l^{-1}$. The critical nutrient load for eutrophication can be larger compared to oligotrophication in case alternative stable states are present (Scheffer and Van Nes 2007). For more details on the methods to define the vulnerability see Appendix D.

Based on the maximum possible epilimnion chlorophyll-a concentrations in combination with the height of the critical nutrient load, 3 levels can be distinguished:

1) Low vulnerability: maximum chlorophyll-a concentrations are **below** eutrophic levels (<20 $\mu g.l^{-1}$) so lakes do not have a critical nutrient load. These lakes have a low vulnerability since algal blooms will be mild.
2) Medium vulnerability: maximum chlorophyll-a concentrations **above** eutrophic levels (>20 $\mu g.l^{-1}$) and critical nutrient loads **above** 0.0025 $gP.m^{-2}.d^{-1}$. These lakes have a medium vulnerability since an exceedance of the critical nutrient load needs relative high nutrient pollution yet ultimately lead to severe algal blooms.
3) High vulnerability: maximum chlorophyll-a concentrations **above** eutrophic levels (>20 $\mu g.l^{-1}$) and critical nutrient loads **below** 0.0025 $gP.m^{-2}.d^{-1}$. These lakes are highly vulnerable since an exceedance of the critical nutrient load occurs at low nutrient pollution and exceedance will lead to severe algal blooms.

Results

We first validated the model output of the VIC-LAKE model (Fig. 3). The regression lines for the VIC-LAKE run were all close to the 1:1 line as can be seen from the intercepts which were close to 0 (−0.81 to 0.06) and slopes which were close to 1 (0.95–0.99) for all 5 regression lines (4 climate models as input and 1 average). The goodness of fit (R^2_{adj}) varies between 0.84–0.87 suggesting a relatively good fit, with a slight underestimation of lake temperatures. The average of VIC-LAKE run with input from 4 climate models reflects the data reasonably well, building trust to use the average output of the 4 climate models in our further analysis.

We identified 19,536 lakes in mainland China (>0.1 km^2) (Fig. 4). Most of these lakes (80%) were in the east, and fewer in the west of China (20%). The majority of the lakes were *polymictic continuous warm* lakes (54%) (Fig. 4a). The second largest group consisted of the *monomictic warm* lakes (32%), followed by the *polymictic discontinuous warm* lakes (7%), the *amictic* and *polymictic continuous cold* lakes (both 3%). The *discontinuous cold, monomictic cold, dimictic* and *meromictic* lakes were the least represented (all less than 1% of the total number of lakes).

The spatial distribution of lakes followed the two distinct climate regions found in China with eastern China accommodating typically the warm lake classes and western China the cold lake classes (Fig. 4b). Also, the adjusted latitude showed a clear distribution (Fig. 5): with rising surface temperatures there is a transition from the colder lake classes (e.g. polymictic continuous cold lakes) to warmer classes (e.g. monomictic warm lakes). The variation around the linear downward trend can be explained by the inter-lake variation in other lake characteristics such as depth and area.

The stratification classes were used to further characterize Chinese

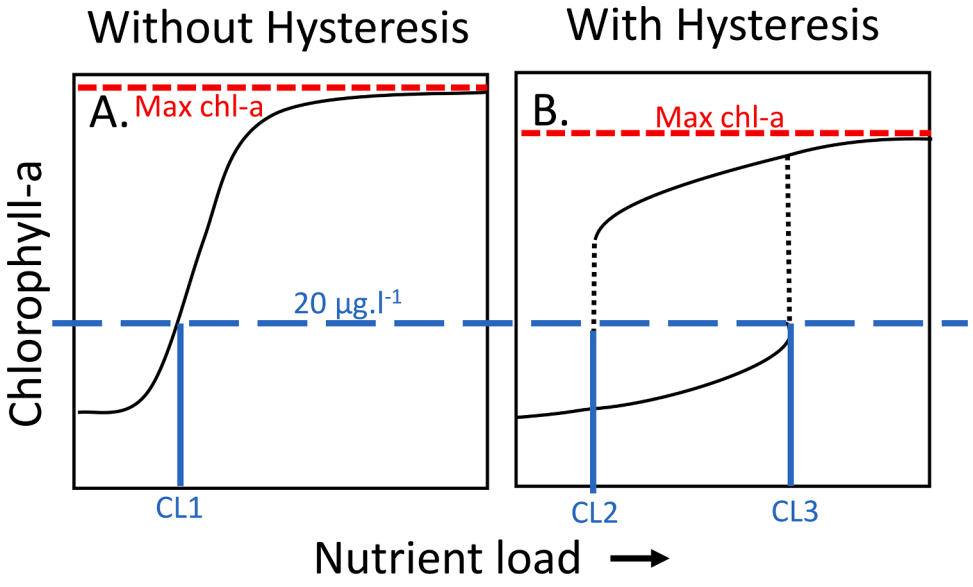

Fig. 2. Examples of load-response curves and related indicators of lake vulnerability. A) a load-response curve without hysteresis (cf. no alternative stable states). B) a load-response curve with hysteresis (cf. with alternative stable states). The maximum chlorophyll-a is indicated with a red dashed line. The critical nutrient load (blue solid line) is calculated as where the load-response curve intersects with the line indicating a threshold of 20 $\mu g.l^{-1}$ chlorophyll-a (blue dashed line). The resulting critical nutrient loads are indicated by CL1 for the load-response curve without hysteresis and CL2 and CL3 for the load-response curve with hysteresis. In the latter case, the critical nutrient load for eutrophication (CL3) is higher than the critical nutrient load for oligotrophication (CL2). (For interpretation of the references to colour in this figure, the reader is referred to the web version of this article.)

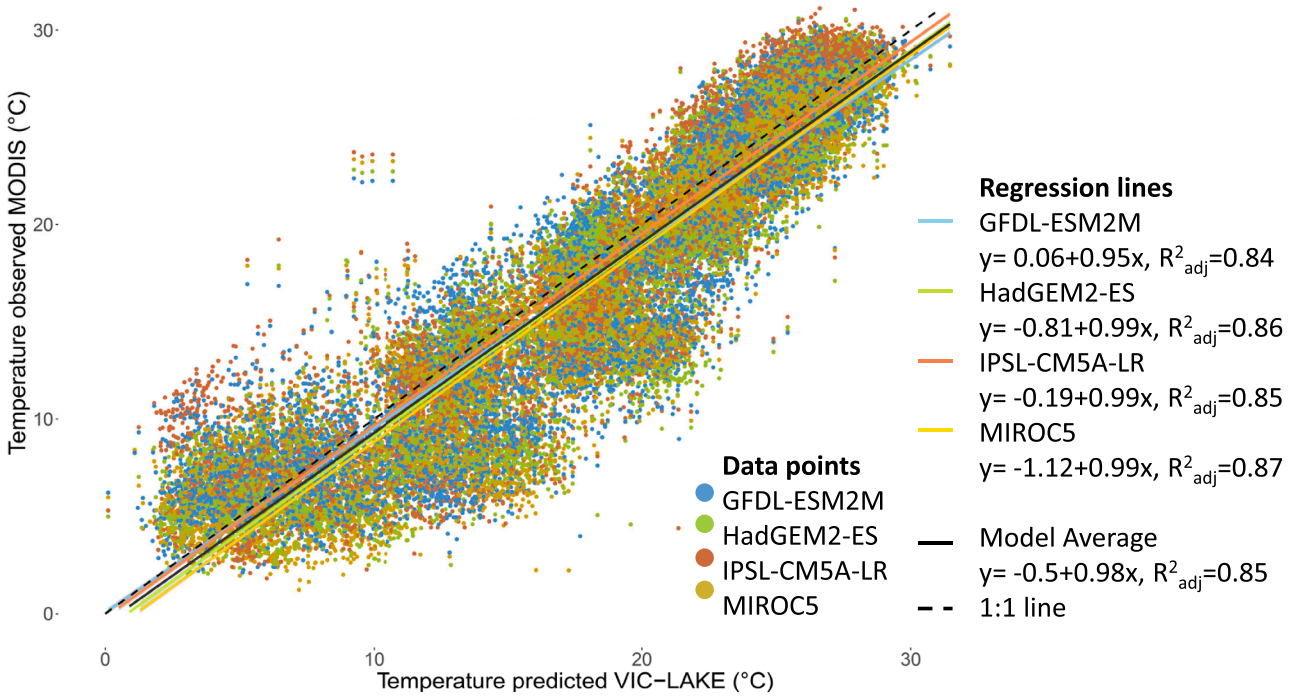

Fig. 3. Comparison of the VIC-LAKE simulated surface water temperature with monthly observations from MODIS (LP DAAC 2020) for 216 lakes in the period 2001–2005. Dots indicate the individual data points (1 lake, 1 day) with different colours referring to the different climate models that were used as input for VIC-LAKE: GFDL-ESM2M (blue), HadGEM2-ES (green), IPSL-CM5A-LR (red) and MIROC5 (yellow). Coloured lines represent the linear regression lines ($y = a+bx$) of observed against modelled water temperature, with their equations provided in the legend. The regression line for the average of the four climate models as input for VIC-LAKE is shown as "Model average" (black solid line). The 1:1 line (dashed black line) reflects a perfect fit that would be reached if all points were on that line ($y = a+bx$ with $a = 0$ and $b = 1$). All p-values were smaller than 0.001. (For interpretation of the references to colour in this figure legend, the reader is referred to the web version of this article.)

lakes based on their morphologic, climate and sediment characteristics (Fig. 5). The Fisher-Pitman Permutation Test showed that the stratification groups were significantly different (all global p-values < 0.001). With the pairwise permutation test, we identified the significant differences between groups of stratification classes.

Although 96% of the lakes in the presented database were relatively shallow with a depth of less than 10 m, we found some differences in morphometry among stratification classes. The *meromictic* and *monomictic warm* lakes seemed slightly deeper and more irregular in shoreline development than the cold lake classes, which was significant for *meromictic* lakes (Fig. 6a&c). The relative deeper warm lakes can be explained by the large proportion of reservoir lakes in the presented database located to the east of China, which tend to be deeper than natural lakes. *Polymictic discontinuous cold* and *monomictic cold* lakes were the shallowest lakes followed by the *polymictic continuous cold* and *polymictic continuous warm* lakes. The *polymictic discontinuous warm* lakes, *amictic* lakes and *dimictic* lakes were slightly deeper.

As the climate parameters were used to group the lakes by stratification class, the climate characterization should logically follow the stratification classes. For the epilimnion and hypolimnion temperatures, the cold lake classes indeed showed the significant lowest temperatures, whereas the warm lake classes showed the significant highest temperatures. Also, ice days showed a significant division among all the lakes, with *amictic lakes* having significantly most ice days. Besides, *Polymictic continuous cold, polymictic discontinuous cold* and *monomictic cold* lakes had significantly more ice days than the warm lake classes.

Temperature differences in the *polymictic continuous cold* and *discontinuous cold* lakes were minute, as these systems are mixed year-round. The *polymictic continuous cold* lakes had a significantly lower epilimnion and hypolimnion temperature compared to the *polymictic continuous warm* lakes. Also, the *polymictic discontinuous cold* lakes had a significantly lower epilimnion and hypolimnion temperature compared to the *polymictic discontinuous warm* lakes (Fig. 6d&e). The *amictic* lakes were significantly distinguished from all other lakes by being nearly permanently ice-covered (Fig. 6f). The epilimnion temperatures in *amictic* lakes were on average 0.5 °C lower than the hypolimnion temperatures, showing inverse stratification. *Meromictic* lakes showed the significant highest epilimnion temperature, yet their hypolimnion waters were significantly colder than the *dimictic* and *monomictic warm* lakes due to the permanent stratification. The *monomictic cold* lakes were similar in temperature and ice-coverage to the *polymictic discontinuous cold* lakes, but they stratified for a longer period. Also, *dimictic* and *monomictic warm* lakes did not differ significantly in terms of their average epilimnion and hypolimnion temperatures but the *monomictic warm* lakes had a single mixing period resulting in higher temperature variation and a larger range in ice days.

Next, we analysed sediment characteristics. Although differences were small, the warm lakes (T_{avg}>4 °C) reach higher maxima clay contents than the cold lakes (Fig. 6g), which was significant for the *meromictic* lakes showing the highest clay content. *Amictic* lakes had the lowest average clay content, though not statistically significant from other lake classes. Most lakes were more or less equal in sand content (Fig. 6h). Also, the differences between reference bulk densities were minute (Fig. 6i) with only a clear pattern for *monomictic warm* and *meromictic* lakes which show a low reference bulk density compared to the other lake classes.

As a final step, we assessed the vulnerability of the stratification classes for the maximum possible chlorophyll-a (severity of algal blooms) and the critical nutrient load (onset of algal blooms). Maximum chlorophyll-a concentrations were largely dependent on lake temperature (Fig. 7a), whereas critical nutrient loads were dependent on both temperature and depth (Fig. 7b). Based on the maximum epilimnion chlorophyll-a concentrations in combination with the critical nutrient load, the lake stratification classes can be grouped in terms of their

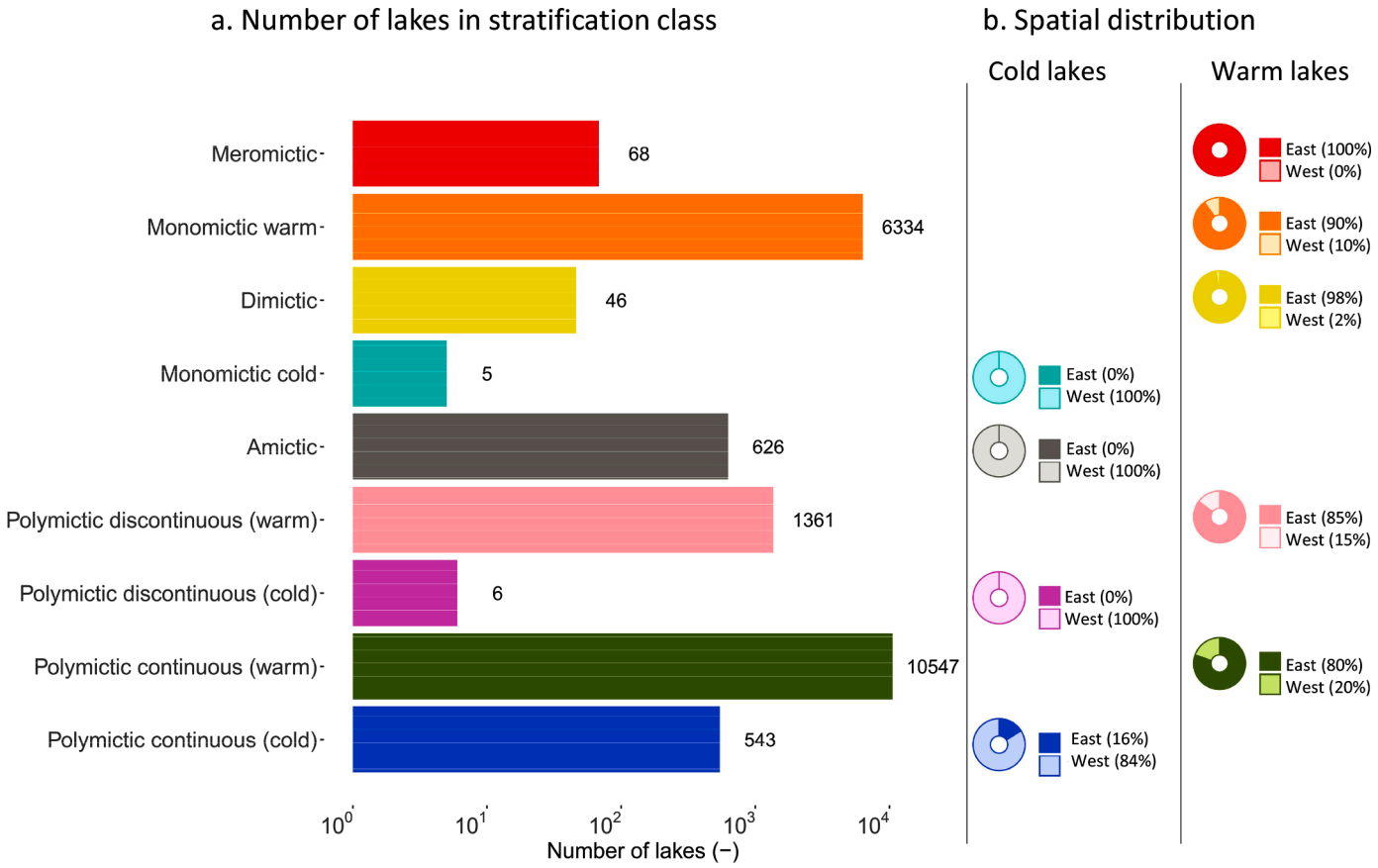

Fig. 4. Number and spatial distribution of stratification classes. (A) Stratification classes for lakes in China (y-axis is on a log-scale). (B) The spatial distribution of lake stratification classes between the west and east of China. $N_{westlakes} = 3994$ (20%) and $N_{eastlakes} = 15{,}542$ (80%). (For interpretation of the references to colour in this figure, the reader is referred to the web version of this article.)

vulnerability to algal bloom formation from low to medium to high:

1 Low vulnerability (max chlorophyll-*a* <20 μg.l^{-1}, no critical nutrient load): *amictic* and *meromictic* lake class. These lakes have low vulnerability as a result of their permanently stratified nature (*meromictic* lakes) or the near-permanently ice-coverage (*amictic*).
2 Medium vulnerability (max chlorophyll-*a* >20 μg.l^{-1}, and critical nutrient loads >0.0025 gP.m^{-2}.d^{-1}): *polymictic continuous warm, polymictic discontinuous cold* and *monomictic cold* lake classes. These lakes showed medium vulnerability as a result of their relatively low depth (<2 m) which initially support macrophytes granting resilience to algal blooms. When nutrient pollution exceeds critical thresholds though, algal blooms will be severe.
3 High vulnerability (max chlorophyll-*a* >20 μg.l^{-1}, and critical nutrient loads <0.0025 gP.m^{-2}.d^{-1}): *polymictic continuous cold, polymictic discontinuous warm, dimictic* and *monomictic warm* lake classes. Except for the *polymictic continuous cold,* these lakes were all highly vulnerable due to their intermediate depth (3.1–5.3 m) and summer temperatures (T>10 °C). Their depth prevents sufficient macrophyte growth to grant resilience to algal blooms and the summer temperatures are ideal for promoting severe algal blooms. Despite being shallower (<2 m depth) *Polymictic continuous cold* lakes also have a high maximum chlorophyll-a and a low critical nutrient load due to the low summer temperatures (T<10 °C). The short growing season of *Polymictic continuous cold* lakes favours fast-growing algae over slower-growing macrophytes.

Discussion

Lake vulnerability to algal bloom formation

We characterized 19,536 Chinese freshwater lakes and identified a spatial division between lakes in the east of China that are typically warmer compared to lakes in the west. Although the majority of the Chinese lakes are shallow with a depth typically less than 10 m, the lakes found in the east of China are slightly deeper compared to their cooler counterparts in the west. Although these spatial patterns in depth might seem counterintuitive, this pattern can be explained by the presence of a large number of reservoir lakes in HydroLAKES in the east of China, which are generally deeper than natural lakes. For sediment, we could not find a clear difference, except for *meromictic* lakes which have significant clay-richer sediment compared to other lakes. Finally, our model results suggest that cold lake classes (*amictic, monomictic cold, polymictic discontinuous cold*) typically seem to have a low to medium vulnerability to algal blooms. An exception forms the *polymictic continuous cold* lakes with a high modelled vulnerability, possibly due to the absence of stratification and the short growing season promoting algae over macrophytes. Moreover, our model results suggest that the warm lake classes (*polymictic continuous warm, polymictic discontinuous warm, dimictic* and *monomictic warm*) seem to have a medium to high vulnerability to algal blooms. An exception forms the *meromictic* lakes with their low modelled vulnerability to algal blooms explained by the permanent stratified nature leading to losses of nutrients to the hypolimnion. The effect of the different morphometric, climate and sediment characteristics on lake vulnerability to the severity and onset of algal blooms is complex because of the various mechanisms through which primary producers are affected; yet some general patterns can be

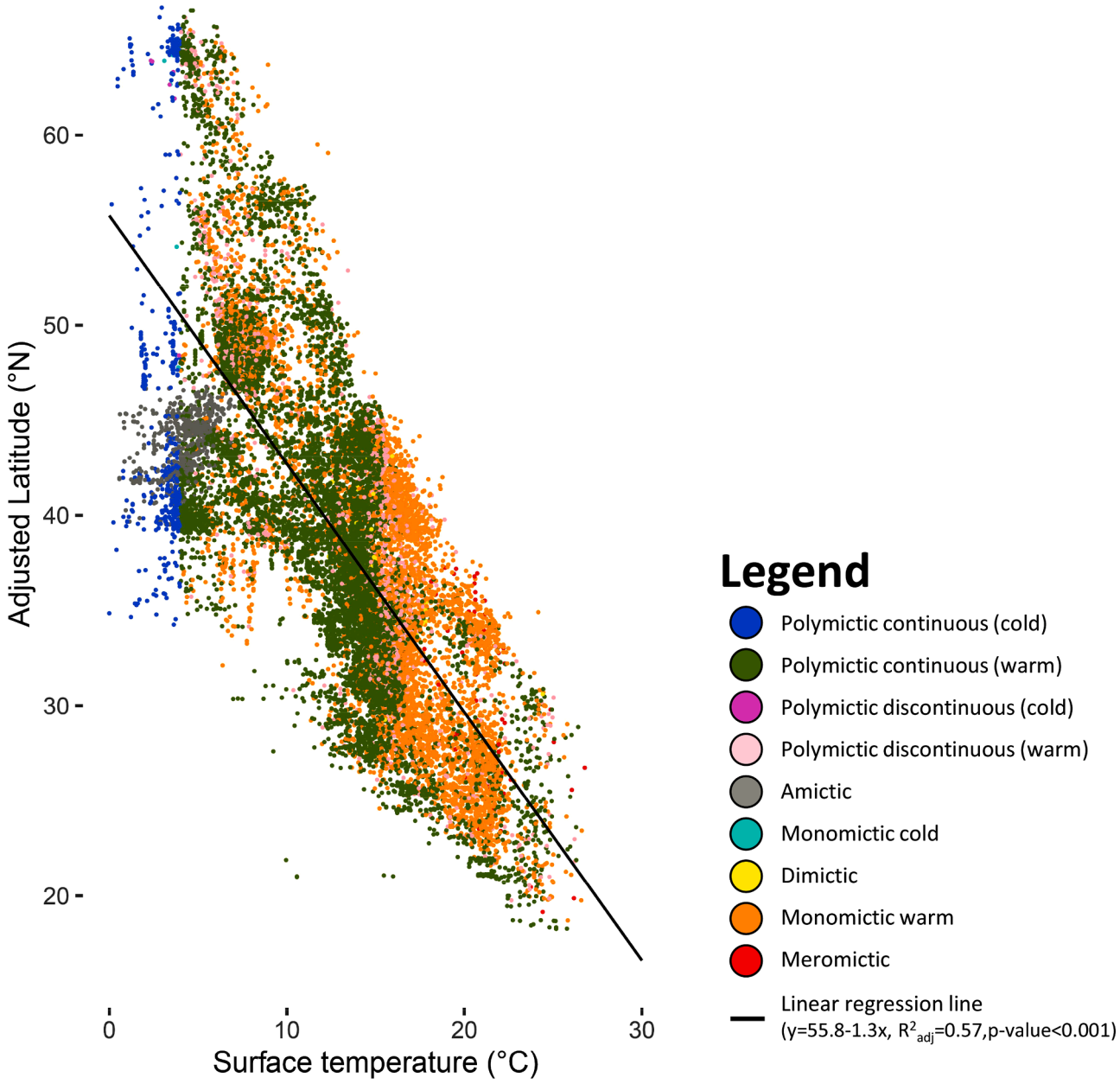

Fig. 5. The average surface lake water temperature as a function of adjusted latitude (altitude corrected latitude). (For interpretation of the references to colour in this figure legend, the reader is referred to the web version of this article.)

derived.

Effect of morphometric characteristics on lake vulnerability

Morphological characteristics of lakes are important factors determining phytoplankton concentrations (Håkanson 2005). We found that the differences among the morphometric characteristics are most profound for lake depth. The lakes in the east of China tend to be slightly deeper because of many deep reservoirs than the cooler lake classes in western China. The effect of depth on the lake vulnerability of algae is not straightforward. Janse et al. (2008) and Scheffer and Van Nes (2007) show that increasing depths in shallow lakes with dense macrophyte biomass result in a lower threshold for nutrient loads leading to an earlier onset of algal blooms. For deeper lakes, however, it is shown that the risk of algal blooms decreases with depth (Håkanson 2005; Liu et al., 2010). Our assessment of lake vulnerability follows this pattern. First, the critical nutrient load was lowest for lakes with the intermediate water level (3–4 m) suggesting that these lakes are most vulnerable to the onset of algal blooms. Both, deeper and shallower lakes showed more resilience to the onset of algal blooms compared to lakes with an intermediate water level.

Effect of climate characteristics on lake vulnerability

For the climate characteristics, we found that the lakes show a clear spatial distribution over China with the warm lake classes in eastern China and the cold lakes in western China. Our model indicated that warm lake classes seem more vulnerable to severe algal blooms confirming previous research (Paerl and Huisman 2008). For instance, low temperatures in *polymictic continuous cold* and *polymictic discontinuous cold* lakes lead to less severe algal blooms compared to, respectively, *polymictic continuous warm* and *polymictic discontinuous warm* lakes. In addition, the vulnerability of lakes to algal blooms also depends on stratification and mixing periods of lakes, which could mobilize or block phosphorus release from the sediments affecting algal blooms (Wetzel

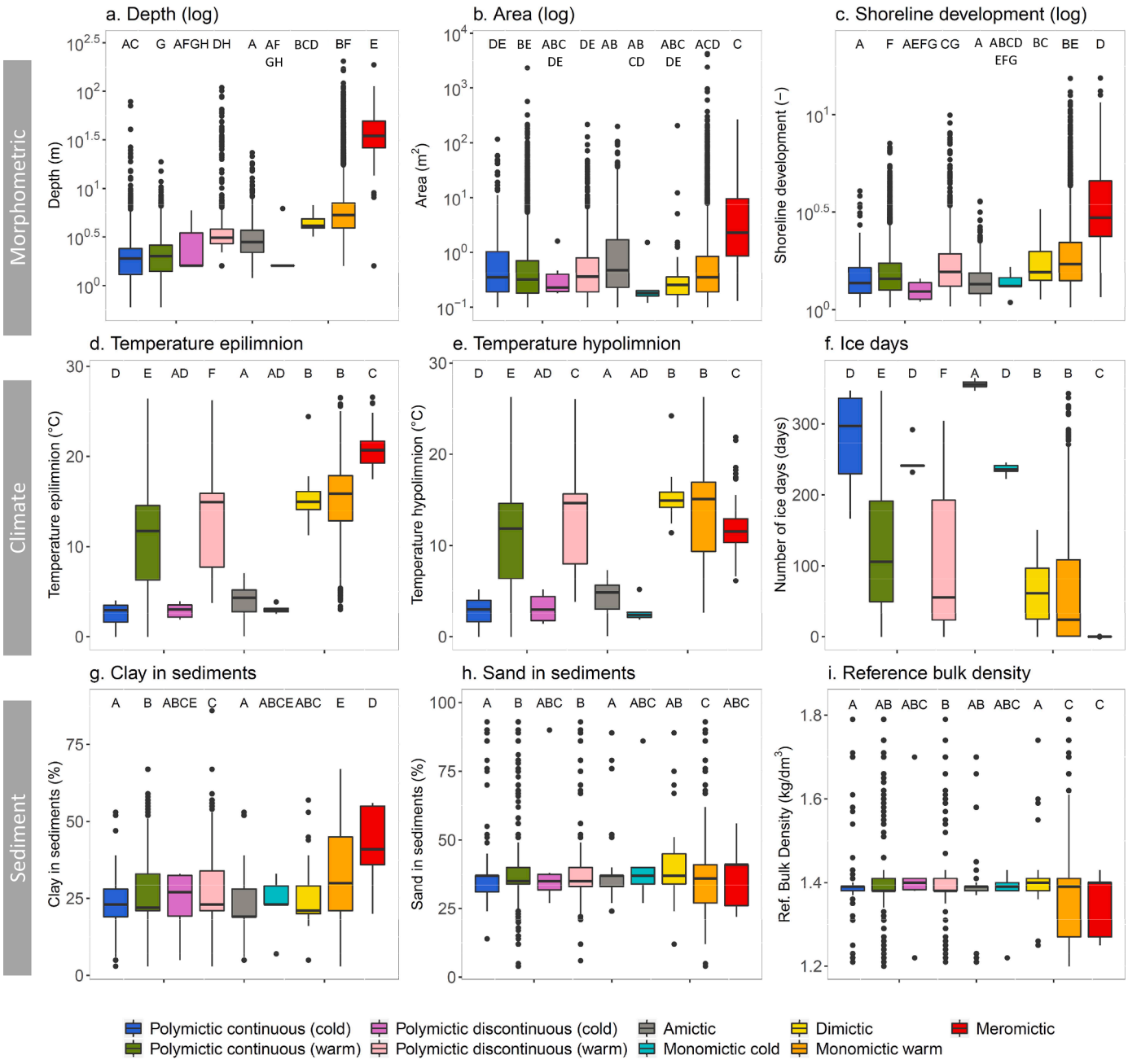

Fig. 6. Characterization of the lakes in China according to their morphometric, climate and sediment characteristics. Morphometric characteristics: (a) Depth, (b) Area, and (c) Shoreline development (ratio between shoreline length and lake surface area); Climate characteristics: (d) Temperature epilimnion, (e) Temperature hypolimnion, (f) Ice days; and Sediment characteristics: (g) Clay content in sediments, (h) Sand content in the sediments and (i) Reference bulk density. The capital letters (A-H) on top of each histogram indicate significantly different groups per characteristic according to the pairwise permutation test ($p<0.05$). Note the log-scale for the morphometric characteristics. (For interpretation of the references to colour in this figure legend, the reader is referred to the web version of this article.)

2001; Wilhelm and Adrian 2008). *Meromictic* lakes hardly mix so that the hypolimnion functions as a nutrient sink, making nutrients unavailable for algal growth (Judd et al., 2005) and resulting in a low vulnerability to severe algal blooms. *Monomictic warm* lakes mix for longer periods. However, since stratification mainly occurs during summer, nutrients availability during the growing season is blocked, leading to less severe algal blooms compared to non-stratifying lakes. *Dimictic* lakes mix and stratify twice a year, supplying algal blooms with sufficient nutrients potentially leading to severe algal blooms. Also, the ice period is important. Under-ice algal growth is typically limited by light, especially when covered with snow. We showed that the long-lasting ice-layer in *amictic* greatly reduces the risk of blooms resulting in a maximum chlorophyll-a concentration of 16 $\mu g.l^{-1}$. This result is in line with Hampton et al. (2017), who found that summer average chlorophyll-a in icy lakes are 13.6 ± 2.84 $\mu g.l^{-1}$. However, in specific cases when light is sufficient, the under-ice environment can be hospitable for algal growth, resulting in higher algal biomasses (Hampton et al., 2017).

Effect of sediment characteristics on lake vulnerability

Finer sediments could be expected at low elevated regions due to a process called "downward fining" (Paola and Seal 1995). We observed a slightly higher maximum clay content in warm lakes than in cold lakes, yet this was only significant for meromictic lakes. Clay is known to bind phosphorus under aerobic conditions and releases phosphorus under anaerobic conditions (Li et al., 2017; Søndergaard et al., 2003). Lakes

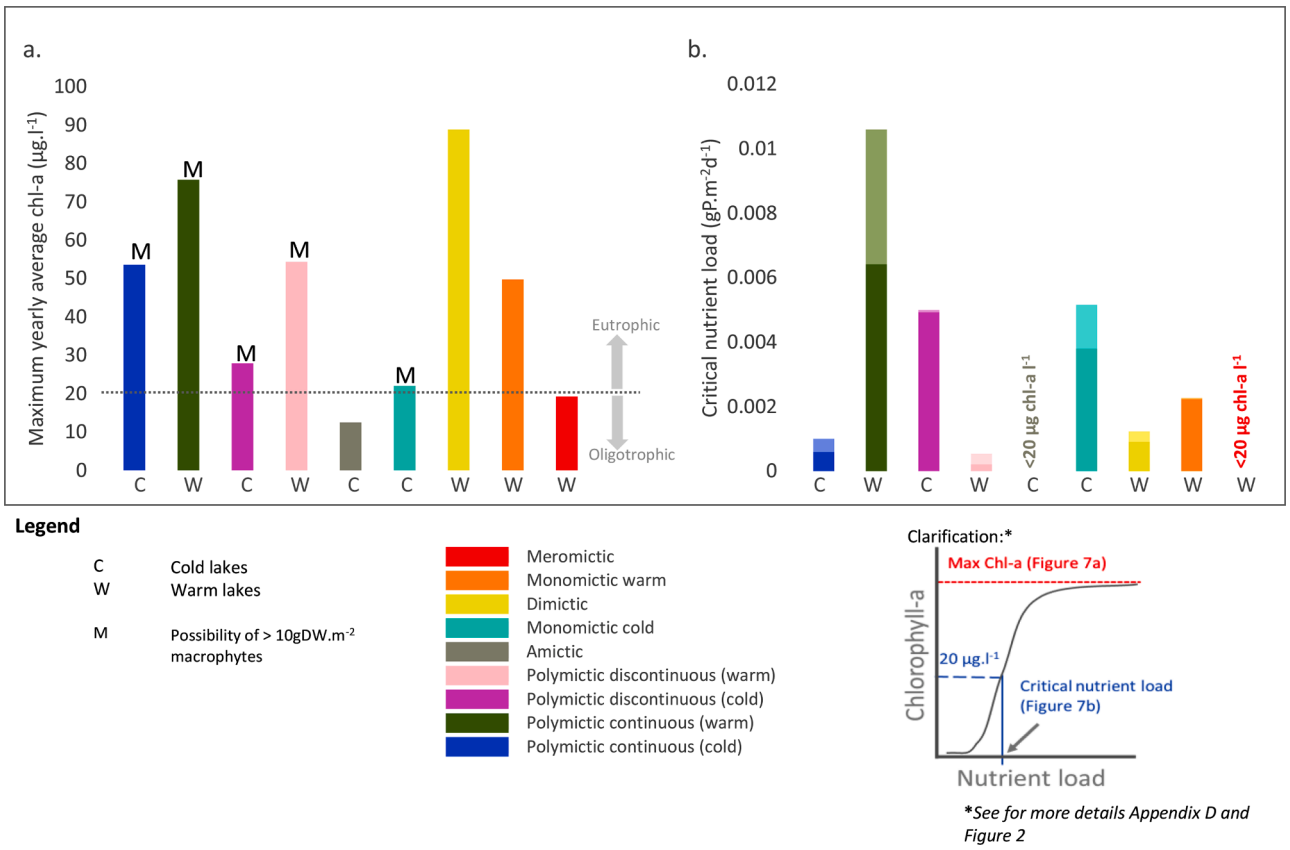

Fig. 7. Vulnerability of lakes to algal bloom formation. a) Vulnerability in terms of maximum yearly average epilimnion algal concentration (µg.l^{-1}), which is reached when algae become light-limited. High algal concentration indicates high vulnerability to the severity of algal blooms. b) Vulnerability in terms of the critical nutrient load (gP.m^{-2}.d^{-1}), which is reached when the lake becomes eutrophic and thus has an algae concentration of 20 µg.l^{-1} or more. High critical nutrient loads or the absence of critical nutrient loads indicate low vulnerability to the onset of algal blooms. Darker colours indicate the critical nutrient load from turbid to clear; lighter colours indicate the critical nutrient load from clear to turbid. If lighter colours are visible, the lake shows alternative stable states. The cold lakes are indicated with a C below the bar and warm lakes with a W below the bar. The M on top of the bars indicate lakes with potential substantial macrophyte growth (>10 gDW.m^{-2}). (For interpretation of the references to colour in this figure legend, the reader is referred to the web version of this article.)

with higher clay contents have typically lower critical nutrient loads meaning that lower nutrient input is needed to trigger algal blooms compared to other lakes (Janse et al., 2008). Since variation in sediment characteristics was larger within stratification classes than between stratification classes, conclusions on the sediment data remained elusive.

Discretizing our world

Here we discretized the lakes by stratification class. Discretization improves the understanding of lake ecosystems, especially in big data studies (Kraemer 2020). Yet, discretization also depends on choices and could in itself create uncertainty. Here, we grouped lakes by stratification classes, using 100 years averaged daily epilimnion and hypolimnion temperatures; hereafter referred to as 'averaging-method'. Alternatively, stratification classes can be based on the most common stratification class among the 100 specific years; hereafter we referred to this as the 'mode-method' (Woolway and Merchant 2019).

Whether the mode- or averaging-method is preferred depends on the goal. Both methods show most lakes are polymictic and indicate that the warm lakes are mainly located in the east and the cold lakes in the west (Appendix E). The mode-method provides information on the dynamics of the stratification class and assigns the most common stratification class, even if this occurs only for 25% of the time. With the averaging-method, the stochasticity in weather patterns is averaged out leading to more stable predictions. With the averaging-method, we obtained logical results along with the stratification classes such as reverse stratification in *amictic* lakes and lower hypolimnion temperatures in *meromictic* lakes. We here think that both methods provide valuable information, but we used the averaging-method in our study to set a baseline of the average stratification classes of the lakes in China.

Data validity

This study provides the first analysis with a comprehensive database that combines morphometric, climate and sediment characteristics of lakes in China. Yet, combining data from different databases could introduce uncertainty in the analysis from the different sources: 1) the morphometric variables from Messager et al. (2016), 2) the climate variables from VIC-LAKE model simulations and 3) the sediment data from FAO/IIASA/ISRIC/ISS-CAS/JRC (2009). To analyze the uncertainty in our study we have recalled uncertainties in the morphometric data (Messager et al., 2016) and validated the climate characteristics and sediment characteristics. We found the largest uncertainty in the sediment parameters, which we validated on a set of European lakes (Appendix B). Validation of our method for China specifically was not possible, as data to do so are currently unavailable to us. Similar to Europe, lake sediment has been disturbed in China due to intensive human activities (e.g. sand dredging, Li et al. (2014)). Therefore, lake sediment layers may be disturbed, leading to uncertainty in this data. Yet, we expect that this uncertainty has a limited impact on our main conclusion, as variations in sediment characteristics between the stratification groups were smaller compared to variation within stratification groups. On the contrary, water temperatures showed a relatively low

uncertainty. The average surface water temperature calculated with VIC-LAKE with the 4 climate models demonstrates an acceptable performance of VIC-LAKE. Although single lake estimates could deviate from this average, we still saw good agreement for specific lakes (Appendix A). Recalling the validity in the morphometric characteristics, Messager et al. (2016) found acceptable uncertainty ranges, yet with less predictive power for smaller lakes compared to larger lakes. Using PCLake+, we assessed the lake vulnerability to algal blooms for representative lakes based on the combined database. PCLake+ is a validated model showing generally an acceptable agreement with lake water quality data (Janse et al., 2010; Janssen et al., 2017; Kong et al., 2016; Li et al., 2019). Given the uncertainty of all data sources, we deem the presented combined database suitable for studies on a national scale, but care should be taken when interpreting the results for individual lakes, as single lake estimates could hold relatively large errors.

Future outlook: Temperature and eutrophication

In this study we presented baseline average stratification classes for Chinese lakes and their characteristics and showed that the most vulnerable lakes to algal blooms are likely located in the east. The east-west distribution of Chinese lake vulnerability coincides with the human population distribution over China, with the densest population in the east and the thinnest populated in the west (Tong et al., 2020; Tong et al., 2017). Human activities tend to cluster in downstream regions (Fang et al., 2018) which are also typically warmer due to the lower elevation. The coincidence of lake vulnerability with the highest human population might seem obvious, yet they do not necessarily share the same cause as humans seek opportunities for trade, transport, and natural resources (Fang et al., 2018), whereas lake vulnerability seems to be related to temperature and lake depth.

The future is likely to change e.g. due to climate and land-use change (Ma et al., 2010; Strokal et al., 2016). Consequently, lake characteristics are also likely to change in the future, changing the future vulnerability to algal blooms of lakes. Climate change will affect future algal growth in two ways. First, lakes are expected to heat up (Vanderkelen et al., 2020) resulting in changes in stratification classes (Woolway and Merchant 2019). The number of ice-covered lakes is likely to decrease and lakes will increasingly stratify (Woolway and Merchant 2019). The magnitude of change depends on the lake characteristics (Kraemer et al., 2015), but lake warming is likely to prolong and intensify algal blooms (Paerl and Huisman 2008; Tong et al., 2021). Second, it is expected that climate change in China will lead to wetter conditions resulting in lower nutrient retentions on land (Wang et al., 2020). As a result, more nutrients will end up in freshwater systems potentially leading to algal blooms.

At the same time stress from eutrophication is likely to increase due to expected socioeconomic developments. Eutrophication is a major concern in China and many lakes are already eutrophic and most profound in the east (Huang et al., 2020; Liu et al., 2010; Tong et al., 2017; Wang et al., 2018). Food production and urbanization are important sources of nutrient losses to the environment (Strokal et al., 2016; Teurlincx et al., 2019). Future socioeconomic development is expected to allow a further increase in eutrophication (Strokal et al., 2014). Besides, N:P ratios in lakes might increase for instance due to improved wastewater treatment (Tong et al., 2019; Tong et al., 2020). This is because phosphorus has, in contrast to nitrogen, no gaseous forms, making it easier to remove it. Elevated N:P ratios may favor blooms of potentially toxic non-N-fixing cyanobacteria (Van de Waal et al. 2014).

Defining future changes in the vulnerability of lakes to algal blooms is beyond the scope of this study. Yet, lake characteristics will likely determine the severity of the algal response. Whereas increasing nutrient loads and N:P ratios together with warmer lake water could result in longer periods of more severe algal blooms, stronger stratification could mitigate this process by functioning as an algal sink. Modeling of future scenarios of socio-ecological development could indicate the directions of future algal bloom developments (Janssen et al., 2019a; Mooij et al., 2019). With this characterization of the Chinese lakes, we aim to contribute to this step.

Conclusions

This study provides the first analysis with a comprehensive database that combines morphometric, climate and sediment characteristics of lakes, including ponds and reservoirs, in China. With this database, we aimed to assess the effect of lake characteristics in Chinese lakes on the vulnerability to algal blooms. We found in this database that lakes, ponds and reservoirs in the east of China are typically warmer and slightly deeper than lakes in the west. Simulations for representative lakes for each stratification class suggest that the warm lakes in the east of China seem to be generally more vulnerable to algal blooms than the cold lakes in the west, with exceptions of the *meromictic* lakes and *polymictic cold* lakes. The unfortunate coincidence that high lake vulnerability is found in the east of China where nutrient pollution is highest asks for priority in preventing severe algal blooms in those regions.

Declaration of Competing Interest

The authors declare that they have no known competing financial interests or personal relationships that could have appeared to influence the work reported in this paper.

Acknowledgments

We would like to thank the anonymous reviewers for providing constructive comments which greatly improved earlier versions of our manuscript. The work of ABGJ is supported by the NWO talent grant Veni (project number VI.Veni.194.002) and the KNAW project SURE+ (PSA-SA-E-01). BD is supported by the Wageningen Institute for Environment and Climate (WIMEK) research grant (grant no. 5160957551). YT is funded by the National Natural Science Foundation of China (no. 41977324). XK is funded by the National Key Research and Development Program of China (2019YFA0607100).

Research data for this article

In this study, we used data for analysis, data for validation and created model and R-scripts. Data used for analysis can be found at 1) morphometric characteristics: Messager et al., 2016, [Creative Commons Attribution 4.0 International License], 2) climate characteristics: https://doi.org/10.4121/13348004 [CC-BY] and 3) sediment characteristics: FAO/IIASA/ISRIC/ISS-CAS/JRC 2009 [Copyright FAO, IIASA, ISRIC, ISSCAS, JRC]. Data for validation can be found at 1) surface water temperature: https://doi.org/10.5067/MODIS/MOD11A1.006 [MODIS data and products acquired through the LP DAAC have no restrictions on subsequent use, sale, or redistribution] and 2) sediments: Janse et al., 2010. R-scripts as well as the model scripts (both VIC-LAKE and PCLAKE+) can be found at https://doi.org/10.4121/13348004 [CC-BY].

Supplementary materials

Supplementary material associated with this article can be found, in the online version, at doi:10.1016/j.watres.2021.117427.

References

Andersson, B., 2001. Macrophyte development and habitat characteristics in Sweden's large lakes. Ambio 30 (8), 503–513.
Aronow, S., 1984. Beaches and Coastal Geology. Springer US, Boston, MA, pp. 754–755.
Bigg, P., 1967. Density of water in SI units over the range 0-40 C. Br. J. Appl. Phys. 18 (4), 521.

Bowling, L.C., Lettenmaier, D.P., 2010. Modeling the Effects of Lakes and Wetlands on the Water Balance of Arctic Environments. J. Hydrometeorol. 11 (2), 276–295.
Carlson, R.E., 1977. A trophic state index for lakes1. Limnol. Oceanogr. 22 (2), 361–369.
Chang, M., Teurlincx, S., DeAngelis, D.L., Janse, J.H., Troost, T.A., van Wijk, D., Mooij, W.M., Janssen, A.B.G., 2019. A generically parameterized model of Lake eutrophication (GPLake) that links field-, lab- and model-based knowledge. Sci. Total Environ., 133887
Chang, N., Zhang, Q., Wang, Q., Luo, L., Wang, X.C., Xiong, J., Han, J., 2020. Current status and characteristics of urban landscape lakes in China. Sci. Total Environ. 712, 135669.
ESRI (2021) World imagery [basemap] ArcGIS Map Service https://services.arcgisonline.com/ArcGIS/rest/services/World_Imagery/MapServer Retrieved at 16 April 2021.
Evans, R.D., 1994. Empirical evidence of the importance of sediment resuspension in lakes. Hydrobiologia 284 (1), 5–12.
Fang, Y., Ceola, S., Paik, K., McGrath, G., Rao, P.S.C., Montanari, A., Jawitz, J.W., 2018. Globally Universal Fractal Pattern of Human Settlements in River Networks. Earth's Future 6 (8), 1134–1145.
FAO/IIASA/ISRIC/ISS-CAS/JRC, 2009. Harmonized World Soil Database (Version 1.1). FAO (ed). Rome, Italy and IIASA, Laxenburg, Austria.
Gao, C., Zhang, T., 2010. Eutrophication in a Chinese Context: understanding Various Physical and Socio-Economic Aspects. Ambio 39 (5), 385–393.
Guan, D., Hubacek, K., 2007. Assessment of regional trade and virtual water flows in China. Ecol. Econ. 61 (1), 159–170.
Håkanson, L., 2005. The importance of lake morphometry for the structureand function of lakes. Int. Rev. Hydrobiol.: J. Covering all Aspects Limnol. Marine Biol. 90 (4), 433–461.
Hampton, S.E., Galloway, A.W.E., Powers, S.M., Ozersky, T., Woo, K.H., Batt, R.D., Labou, S.G., O'Reilly, C.M., Sharma, S., Lottig, N.R., Stanley, E.H., North, R.L., Stockwell, J.D., Adrian, R., Weyhenmeyer, G.A., Arvola, L., Baulch, H.M., Bertani, I., 2017. Ecol. Under Lake Ice. Ecol. Lett. 20 (1), 98–111.
Hostetler, S.W., 1991. Simulation of lake ice and its effect on the late-Pleistocene evaporation rate of Lake Lahontan. Clim. Dyn. 6 (1), 43–48.
Hostetler, S.W., Bartlein, P.J., 1990. Simulation of lake evaporation with application to modeling lake level variations of Harney-Malheur Lake. Oregon. Water Resour. Res. 26 (10), 2603–2612.
Hothorn, T., Hornik, K., van de Wiel, M.A., Zeileis, A. and Hothorn, M.T. (2019) Package 'coin'.
Huang, J., Zhang, Y., Arhonditsis, G.B., Gao, J., Chen, Q., Peng, J., 2020. The magnitude and drivers of harmful algal blooms in China's lakes and reservoirs: a national-scale characterization. Water Res. 181, 115902.
ISIMIP (2020) Inter-Sectoral Impact Model Intercomparison Project. https://www.isimip.org/.
Janse, J.H., De Senerpont Domis, L.N., Scheffer, M., Lijklema, L., Van Liere, L., Klinge, M., Mooij, W.M., 2008. Critical phosphorus loading of different types of shallow lakes and the consequences for management estimated with the ecosystem model PCLake. Limnologica-Ecol. Manage. Inland Waters 38 (3), 203–219.
Janse, J.H., Scheffer, M., Lijklema, L., Van Liere, L., Sloot, J.S., Mooij, W.M., 2010. Estimating the critical phosphorus loading of shallow lakes with the ecosystem model PCLake: sensitivity, calibration and uncertainty. Ecol. Modell. 221 (4), 654–665.
Janssen, A.B.G., de Jager, V.C.L., Janse, J.H., Kong, X., Liu, S., Ye, Q., Mooij, W.M., 2017. Spatial identification of critical nutrient loads of large shallow lakes: implications for Lake Taihu (China). Water Res. 119, 276–287.
Janssen, A.B.G., Hilt, S., Kosten, S., de Klein, J., Paerl, H.W., Van de Waal, D.B., 2020. Shifting states, shifting services: linking regime shifts to changes in ecosystem services of shallow lakes. Freshw. Biol. 66 (1), 1–12.
Janssen, A.B.G., Janse, J.H., Beusen, A.H.W., Chang, M., Harrison, J.A., Huttunen, I., Kong, X., Rost, J., Teurlincx, S., Troost, T.A., van Wijk, D., Mooij, W.M., 2019a. How to model algal blooms in any lake on earth 36, 1–10. Current Opinion in Environmental Sustainability.
Janssen, A.B.G., Teurlincx, S., An, S., Janse, J.H., Paerl, H.W., Mooij, W.M., 2014. Alternative stable states in large shallow lakes? J. Great Lakes Res. 40 (4), 813–826.
Janssen, A.B.G., Teurlincx, S., Beusen, A.H.W., Huijbregts, M.A.J., Rost, J., Schipper, A. M., Seelen, L.M.S., Mooij, W.M., Janse, J.H., 2019b. PCLake+: a process-based ecological model to assess the trophic state of stratified and non-stratified freshwater lakes worldwide. Ecol. Modell. 396, 23–32.
Judd, K.E., Adams, H.E., Bosch, N.S., Kostrzewski, J.M., Scott, C.E., Schultz, B.M., Wang, D.H., Kling, G.W., 2005. A case history: effects of mixing regime on nutrient dynamics and community structure in third sister lake, michigan during late winter and early spring 2003. Lake Reserv. Manag. 21 (3), 316–329.
Kong, X., He, Q., Yang, B., He, W., Xu, F., Janssen, A.B.G., Kuiper, J.J., Van Gerven, L.P. A., Qin, N., Jiang, Y., Liu, W., Yang, C., Bai, Z., Zhang, M., Kong, F., Janse, J.H., Mooij, W.M., 2016. Hydrological regulation drives regime shifts: evidence from paleolimnology and ecosystem modeling of a large shallow Chinese lake. Glob. Chang Biol. 23 (2), 737–754.
Kraemer, B.M., 2020. Rethinking discretization to advance limnology amid the ongoing information explosion. Water Res. 178, 115801.
Kraemer, B.M., Anneville, O., Chandra, S., Dix, M., Kuusisto, E., Livingstone, D.M., Rimmer, A., Schladow, S.G., Silow, E., Sitoki, L.M., Tamatamah, R., Vadeboncoeur, Y., McIntyre, P.B., 2015. Morphometry and average temperature affect lake stratification responses to climate change. Geophys. Res. Lett. 42 (12), 4981–4988.
Lewis Jr, W.M., 1983. A revised classification of lakes based on mixing. Can. J. Fish. Aquat.Sci. 40 (10), 1779–1787.
Li, J., Fei, L., Chen, Z., Sun, X., 2017. Particle size distribution and settling velocity of sediments in water diverted from the Yellow River during border-strip irrigation. Tecnología y ciencias del agua 8 (2), 31–41.
Li, J., Tian, L., Chen, X., Li, X., Huang, J., Lu, J., Feng, L., 2014. Remote-sensing monitoring for spatio-temporal dynamics of sand dredging activities at Poyang Lake in China. Int. J. Remote Sens. 35 (16), 6004–6022.
Li, X., Janssen, A.B.G., de Klein, J.J.M., Kroeze, C., Strokal, M., Ma, L., Zheng, Y., 2019. Modeling nutrients in Lake Dianchi (China) and its watershed. Agric. Water Manage. 212, 48–59.
Liu, W., Zhang, Q., Liu, G., 2010. Lake eutrophication associated with geographic location, lake morphology and climate in China. Hydrobiologia 644 (1), 289–299.
LP DAAC (2020) MOD11A1.006 Terra Land Surface Temperature and Emissivity Daily Global 1km.
Ma, R., Duan, H., Hu, C., Feng, X., Li, A., Ju, W., Jiang, J., Yang, G., 2010. A half-century of changes in China's lakes: global warming or human influence? Geophys. Res. Lett. 37 (24).
Mangiafico, S., Mangiafico, M.S., 2017. Package 'rcompanion'. Cran Repos 1–71.
Messager, M.L., Lehner, B., Grill, G., Nedeva, I., Schmitt, O., 2016. Estimating the volume and age of water stored in global lakes using a geo-statistical approach. Nat. Commun. 7.
Millero, F.J., Poisson, A., 1981. International one-atmosphere equation of state of seawater. Deep Sea Research Part A. Oceanogr. Res. Papers 28 (6), 625–629.
Mishra, V., Cherkauer, K.A., Bowling, L.C., 2011. Changing thermal dynamics of lakes in the Great Lakes region: role of ice cover feedbacks. Glob. Planet Change 75 (3), 155–172.
Mooij, W.M., van Wijk, D., Beusen, A.H.W., Brederveld, R.J., Chang, M., Cobben, M.M.P., DeAngelis, D.L., Downing, A.S., Green, P., Gsell, A.S., Huttunen, I., Janse, J.H., Janssen, A.B.G., Hengeveld, G.M., Kong, X., Kramer, L., Kuiper, J.J., Langan, S.J., Nolet, B.A., Nuijten, R.J.M., Strokal, M., Troost, T.A., van Dam, A.A., Teurlincx, S., 2019. Modeling water quality in the Anthropocene: directions for the next-generation aquatic ecosystem models. Curr. Opin. Environ. Sustain. 36, 85–95.
Paerl, H.W., Huisman, J., 2008. Blooms like it hot. Science 320 (5872), 57.
Paola, C., Seal, R., 1995. Grain Size Patchiness as a Cause of Selective Deposition and Downstream Fining. Water Resour. Res. 31 (5), 1395–1407.
Patterson, J.C., Hamblin, P.F., 1988. Thermal simulation of a lake with winter ice cover. Limnol. Oceanogr. 33 (3), 323–338.
Piñeiro, G., Perelman, S., Guerschman, J.P., Paruelo, J.M., 2008. How to evaluate models: observed vs. predicted or predicted vs. observed? Ecol. Modell. 216 (3), 316–322.
Qin, B., Zhou, J., Elser, J.J., Gardner, W.S., Deng, J., Brookes, J.D., 2020. Water Depth Underpins the Relative Roles and Fates of Nitrogen and Phosphorus in Lakes. Environ. Sci. Technol. 54 (6), 3191–3198.
Robinson, N., Regetz, J., Guralnick, R.P., 2014. EarthEnv-DEM90: a nearly-global, void-free, multi-scale smoothed, 90m digital elevation model from fused ASTER and SRTM data. ISPRS J. Photogramm. Remote Sens. 87, 57–67.
Schäfer, A.E., Marchett, C.A., Schuh, S.M., Ahlert, S., Lanzer, R.M., 2014. Morphological characterization of eighteen lakes of the north and middle coast of Rio Grande do Sul. Brazil. Acta Limnologica Brasiliensia 26 (2), 199–214.
Scheffer, M., 2004. Ecology of Shallow Lakes. Springer.
Scheffer, M., Van Nes, E.H., 2007. Shallow lakes theory revisited: various alternative regimes driven by climate, nutrients, depth and lake size. Shallow Lakes in a Changing World 196 (1), 455–466.
Søndergaard, M., Jensen, J.P., Jeppesen, E., 2003. Role of sediment and internal loading of phosphorus in shallow lakes. Hydrobiologia 506 (1), 135–145.
Strokal, M., Ma, L., Bai, Z., Luan, S., Kroeze, C., Oenema, O., Velthof, G., Zhang, F., 2016. Alarming nutrient pollution of Chinese rivers as a result of agricultural transitions. Environ. Res. Lett. 11 (2), 024014.
Strokal, M., Yang, H., Zhang, Y., Kroeze, C., Li, L., Luan, S., Wang, H., Yang, S., Zhang, Y., 2014. Increasing eutrophication in the coastal seas of China from 1970 to 2050. Mar. Pollut. Bull. 85 (1), 123–140.
Teurlincx, S., Kuiper, J.J., Hoevenaar, E.C.M., Lurling, M., Brederveld, R.J., Veraart, A.J., Janssen, A.B.G., Mooij, W.M., de Senerpont Domis, L.N., 2019. Towards restoring urban waters: understanding the main pressures 36, 49–58. Current Opinion in Environmental Sustainability.
Tong, Y., Li, J., Qi, M., Zhang, X., Wang, M., Liu, X., Zhang, W., Wang, X., Lu, Y., Lin, Y., 2019. Impacts of water residence time on nitrogen budget of lakes and reservoirs. Sci. Total Environ. 646, 75–83.
Tong, Y., Wang, M., Peñuelas, J., Liu, X., Paerl, H.W., Elser, J.J., Sardans, J., Couture, R.-M., Larssen, T., Hu, H., Dong, X., He, W., Zhang, W., Wang, X., Zhang, Y., Liu, Y., Zeng, S., Kong, X., Janssen, A.B.G., Lin, Y., 2020. Improvement in municipal wastewater treatment alters lake nitrogen to phosphorus ratios in populated regions. Proc. Natl. Acad. Sci. 117 (21), 11566–11572.
Tong, Y., Xu, X., Qi, M., Sun, J., Zhang, Y., Zhang, W., Wang, M., Wang, X., Zhang, Y., 2021. Lake warming intensifies the seasonal pattern of internal nutrient cycling in the eutrophic lake and potential impacts on algal blooms. Water Res. 188, 116570.
Tong, Y., Zhang, W., Wang, X., Couture, R.-M., Larssen, T., Zhao, Y., Li, J., Liang, H., Liu, X., Bu, X., He, W., Zhang, Q., Lin, Y., 2017. Decline in Chinese lake phosphorus concentration accompanied by shift in sources since 2006. Nat. Geosci. 10, 507.
Van de Waal, D.B., Smith, V.H., Declerck, S.A., Stam, E.C., Elser, J.J., 2014. Stoichiometric regulation of phytoplankton toxins. Ecol. Lett. 17 (6), 736–742.
Vanderkelen, I., van Lipzig, N.P.M., Lawrence, D.M., Droppers, B., Golub, M., Gosling, S. N., Janssen, A.B.G., Marcé, R., Schmied, H.M., Perroud, M., Pierson, D., Pokhrel, Y., Satoh, Y., Schewe, J., Seneviratne, S.I., Stepanenko, V.M., Tan, Z., Woolway, R.I., Thiery, W., 2020. Global Heat Uptake by Inland Waters. Geophys. Res. Lett. 47 (12), e2020GL087867.

Wang, M., Kroeze, C., Strokal, M., van Vliet, M.T., Ma, L., 2020. Global change can make coastal eutrophication control in China more difficult. Earth's Future 8 (4), e2019EF001280.
Wang, M., Ma, L., Strokal, M., Ma, W., Liu, X., Kroeze, C., 2018. Hotspots for Nitrogen and Phosphorus Losses from Food Production in China: a County-Scale Analysis. Environ. Sci. Technol. 52 (10), 5782–5791.
Wang, M., Strokal, M., Burek, P., Kroeze, C., Ma, L., Janssen, A.B.G., 2019. Excess nutrient loads to Lake Taihu: opportunities for nutrient reduction. Sci. Total Environ. 664, 865–873.
Wetzel, R.G., 2001. Limnology (Third Edition). Academic Press, San Diego.
Wilhelm, S., Adrian, R., 2008. Impact of summer warming on the thermal characteristics of a polymictic lake and consequences for oxygen, nutrients and phytoplankton. Freshw. Biol. 53 (2), 226–237.
Woolway, R.I., Merchant, C.J., 2019. Worldwide alteration of lake mixing regimes in response to climate change. Nat. Geosci. 12 (4), 271–276.
World Bank (2017) World Bank Staff Estimates Based on Age/Sex Distributions of United Nations Population Division's World Population Prospects: 2019 Revision.